Spectral and Electrical Investigations of Zirconium Doped 212– Bi- Sr-Vanadate Ceramics

Khaled M. Elsabawy*

Materials Science Unit-Chemistry Department-Faculty of Science-31725-Tanta University-Egypt
Materials Science Unit,Faculty of Science,Taif University-Taif City-Alhawyah-888-Saudi Arabia

Abstract : Thepresent investigation study the synthesis of formula $Bi_2SrV_{2-x}Zr_xO_9$, where (x= 0.05, 0.1, 0.2, 0.3, 0.6) which was carefully synthesized and processed by using solid state reaction route and sintering temperature at 850^oC for 10 hrs. XRD – analysis of the prepared samples proved that zirconium-dopant can substitute successfully until x = 0.6 mole on the Bi-layered perovskite crystal structure. Zr - dopings have slight effects on both ESR-signals and conduction mechanism of Zr-doped Bi-Sr-VO regime. Electrical measurements indicated that the energy gap E_g and number of electrons in conduction band N_{cb} increase as the ratio of Zr doping increases from x = 0.05 till x = 0.6 mole respectively .

Keywords: 212-Bi-Vanadates; Zr – Doping ; Perovskite; Ceramic; X- ray; ESR; IR.

Introduction:

The bismuth – oxide layered perovskite materials such as Bi-Sr-V-O have attracted increasing attention in the research community because they are fatigue – free and lead free [1-3].

The wide spread application and commercialization of bismuth- layered perovskite ferroelectrics have been limited by drawbacks, their rather high processing temperature and their relatively low remanent polarization [4-5]. Recently, efforts have been made to enhance the properties of layered perovskite ferroelectrics by addition or substitution of alternative cations [6-8]. It's now well established that the variation of oxygen content and distribution of oxygen atoms on the lattice site strongly influences the physical and structural properties (e.g. electrical conductivity) at high-temperature. Superconductors and many other metallic oxides [9].

The discovery of high temperature superconductors has attracted much attention for their technological application such as superconducting quantum interference devices (SQUID), The high Tc ceramic super-conductor, the Bi –based system has been studied because of its high critical temperature especially with the partial substitution of Pb in Bi and Sr sites since it promotes the stabilization of 2223 phase when grown from 2212 phase [10-11].

Many published papers [12-14] are explaining the discovery of mixed metal oxides having bismuth layer alternating with perovskite structure layers, because of their ionic structural framework, Aurivillius phases exhibit great flexibility with respect to metal cation substitution. Therefore, these phases have high potential for systematic control of their properties [15].

There are different studies showing the chemical substitution such as Pb doping on Bi-O layers that can be used to improve conduction in the blocking layers and so to a large decrease in the resistivity anisotropy. The reduced anisotropy leads to improvement of the critical current in the heavy Pb-doped [16-21].

Das et al. [22] reported the improved remanent polarization of SBN and $SrBi_2Ta_2O_9$ this films, when a small amount of Ca cations were incorporated into A sites: Bismuth layered perovskite materials have high fatigue resistance [23,24] .

The crystal structure and chemical composition of these layered perovskites were systematically studied [25] with the general formula of $(Bi_2O_2)^{2+}$ $(Am^{-1}BmO^3m^{+1})^{3-}$,consisting of m-perovskite unites sandwiched between bismuth oxide layers called the family of bismuth layered structured ferroelectrics [26], where A and B two types of cations that enter the perovskite unite A is Bi^{3+} , Ba^{2+} , Sr^{2+} , and B is Ti^{4+},Ta^{5+} , and m=1-6 layered perovskite strontium tantalite is a member of bismuth layer- structured ferroelectrics.

The crystal structure of Sr $Bi_2Ta_2O_9$ comprises pseudo- perovskite blocks $(SrTa_2O_7)^{2-}$ that are sandwiched between $(Bi_2O_2)^{2+}$ layers. Sr occupies the A site of the perovskite block and Ta occupies the B-site [27].

The essential goal of the present article is to investigate wide range of Zr – dopings on- vanadium sites of 212 Bi-Sr-V-O regime on;

(a) Structural properties.

(b) Spectroscopic properties (IR, ESR).

(c) Conduction behaviour of 212-Bi-Sr-V-O, system.

Experimental:

The pure $Bi_2SrV_2O_9$ and doped samples with the general formula $Bi_2SrV_{2-x}Zr_xO_9$, where x = 0.05, 0.1, 0.2, 0.3, 0.6 mole were prepared by conventional solid state reaction route and sintering procedure using the appropriate amounts of $Bi_2(CO_3)_3$, $SrCO_3$, $(NH_4)_2VO_3$ and ZrO_2 (each purity >99%). The mixture was ground in an agate mortar for one hour. Then the finely ground powder was subject to firing at 800 ^{o}C for 10 hours, reground and finally pressed into pellets with thickness 0.2 cm, diameter 1.2 cm and Sintered at 850 ^{o}C for 10 hours. Then the furnace is cooled slowly down to room temperature. Finally the materials are kept in vacuum desiccator over silica gel dryer.

Structural Measurements:

X-Ray diffraction (XRD):

The X-ray diffraction measurements (XRD) were carried out at room temperature on the fine ground $Bi_2SrV_2O_9$ and $Bi_2SrV_{2-x}Zr_xO_9$ systems in the range (2θ =10-70°) using Cu-Kα radiation source and a computerized [Bruker Axs-D8 advance] X-ray diffractometer with two theta scan technique.

Conductivity Measurements:

The DC-electrical conductivity of the samples was measured using the two terminals DC-method. The pellets were inserted between spring loaded copper electrodes, A KEITHLEY 175 multimeter (ASA) was employed from room temperature up to 500K. The temperature was measured by a calibrated chromel-alumel thermocouple placed firmly at the sample. Measurements were conducted in such a way that at each temperature, sufficient time was allowed to attain thermal equilibration.

Solid infrared absorption spectral measurements:

The IR absorption spectra of the prepared samples were recorded using " Nexus 670 FT IR spectrometer in the range 500-2500 cm-1 using pure KBr matrix".

Electron paramagnetic resonance measurements:

The electron spin resonance spectra (ESR) were recorded at room temperature for the prepared samples using at x-band frequencies on a "Bruker- ELEXSYS E 500 Germany" spectrometer .

Results & Discussion

X-Ray Diffraction:

The X-ray diffraction patterns of pure and Zr-doped samples with the general formula $Bi_2SrV_{2-x}Zr_xO_9$, where x= 0.05, 0.1, 0.2, 0.3, 0.6 mole are shown in Fig (1_{a-f}).
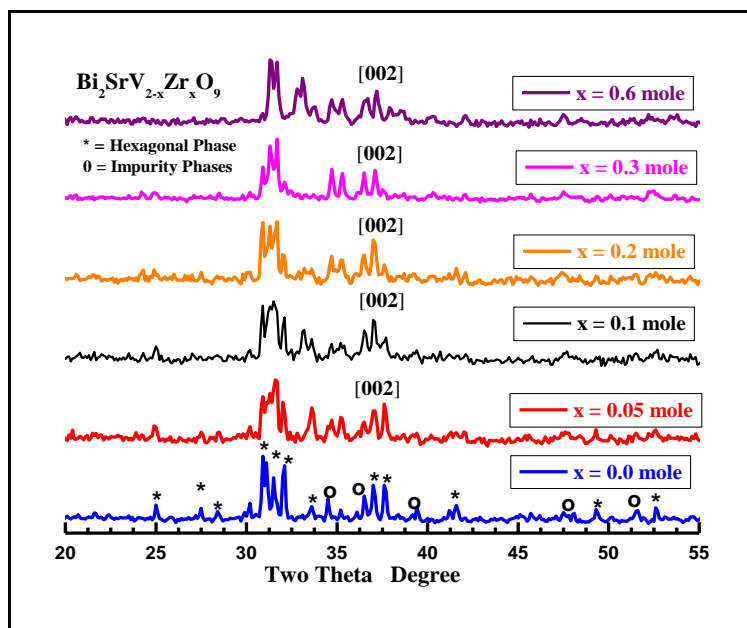
Fig (1$_{a-f}$): XRD patterns recorded for (a) pure Bi$_2$SrV$_2$O$_9$ and Zr-doped samples (b):Bi$_2$SrV$_{1.95}$ Zr $_{0.05}$ O$_9$, (c):Bi$_2$SrV$_{1.9}$ Zr $_{0.1}$ O$_9$,(d): Bi$_2$SrV$_{1.8}$ Zr $_{0.2}$ O$_9$, (e):Bi$_2$SrV$_{1.7}$ Zr $_{0.3}$O$_9$,(f):Bi$_2$SrV$_{1.4}$ Zr$_{0.6}$O$_9$

Analysis of the corresponding 2θ values and the interplanar spacing d (A^o) by using computerized program proved that the compound is mainly belongs to distorted perovskite type with hexagonal crystal form, that expressed by assigned peaks in major . The unite cell dimensions were calculated using parameters of the most intense X-ray reflection peaks and found to be a= b= 5.7804 A^o and c= 7.104A^o for the pure   212Bi-Sr-V-O. Single phase of the layered perovskite structure appeared when Zr is up to or equal 0.05 [28]. The substitution of Zr^{4+} for V^{5+} in BSV would induce A-site cation vacancies in perovskite layers, which leads to an increase of internal stress for the shrinkage of unite cell volume [29]. The increasing of Zr ions in the crystal lattice of BSV will result in strong stress, which will expel other Zr -ions from the crystal lattice of BSV(212-Bi-V-O).

The layered perovskite structure would be more restrictive since (Bi$_2$O$_2$)$^{2+}$ interlayeres impose a great constraint for structural relaxation. Such a structural constraint induced from (Bi$_2$O$_2$)$^{2+}$ interlayeres may well explain the lack of an appreciable decrease in lattice parameters with an increased amount of vanadium dopping [30].
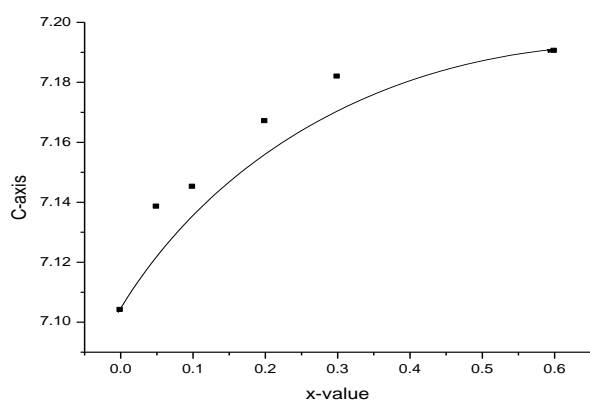

Fig.(2): Variation of *c-axis* as a function of Zr-content .

From Fig.(2) It is clear that *c-axis* increases as result of substitution Zr- dopant on the bases of ionic radius it is expected that *c-axis* increases as Zr^{4+} doping ratio increases. Furthermore, Zr^{4+} is lower in charge than V^{5+} and as a result it is expected to decrease stress inside lattice and consequently the shrinkage factor of lattice will be increased.   From Fig.(1$_{a-f}$), It is clear that the Zr- substitutions are successful in the most of

investigated range even at high concentration x = 0.6 mole since there is no evidence noticeable at X-ray diffractogram referring to Zr- impurity phase. This confirms that Zr-dopant can substitute in the V-sites successfully in the whole investigated range.

Electron paramagnetic resonance measurements:

Fig ($3_{a,c,e}$) explain the electron spin resonance (ESR) signals recorded for pure Bi212 and some selected Zr doped samples with x= 0.1, 0.3 mole.
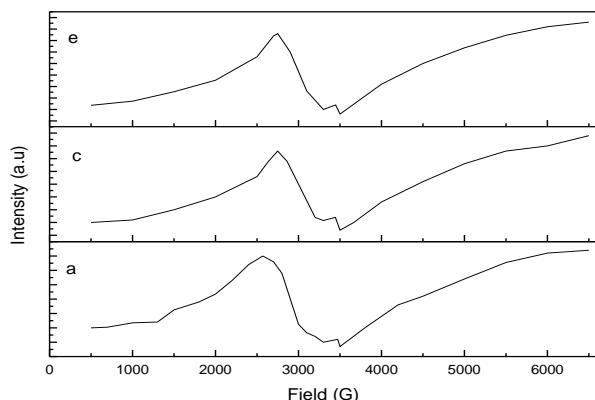

Fig ($3_{a,c,e}$): ESR spectra at room temperature for pure and some selected Zr-doped 212-Bi-Sr-V-O system where (a): $Bi_2SrV_2O_9$, (c): $Bi_2SrV_{1.9}Zr_{0.1}O_9$ and (e): $Bi_2SrV_{1.7}Zr_{0.3}O_9$

It was shown that the effective g-values (g_{iso}) exhibit an increase from x= 0.0 mole to x = 0.3 mol due to strong coupling between Zr^{4+} ion that substitutes V^{5+} ion successfully at low dopant concentration Fig.(4). These results of ESR proved that the anisotropy occurred as a result of Zr doping where g_{eff} varies as function ofx value [31-32].
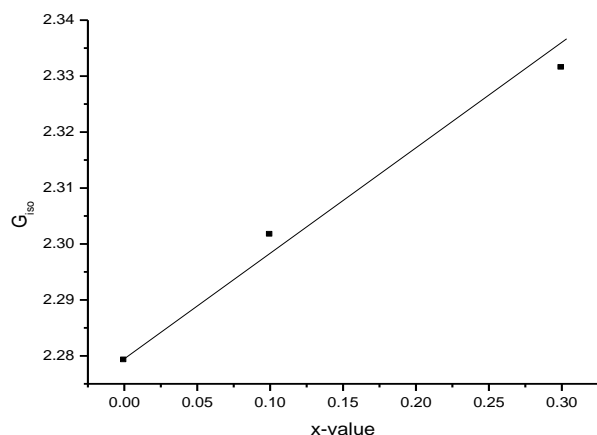

Fig.(4): Variatio of G_{iso} versus x-values .

DC-Electrical conductivity measurements:

Fig.(5_{a-f}) displays the variation of DC-electrical conductivity as a function of reciprocal of absolute temperature for various Zr^{4+} dopings. The data from Fig. (5_{a-f}) exhibit conducting and semiconductor behavior since the conductivity increases as the temperature rise in case of conductor and the conductivity decrease as the temperature rise in case of semiconductor. [33].
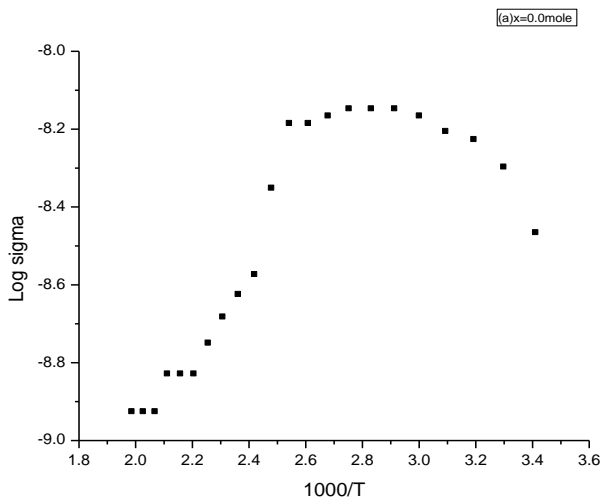
Fig.(5a): Variation of DC- electrical conductivity as a function of temperature for pure 212-Bi-Sr-V-O system .
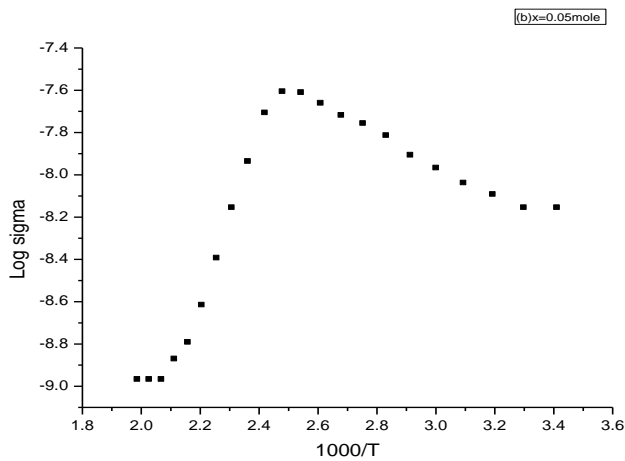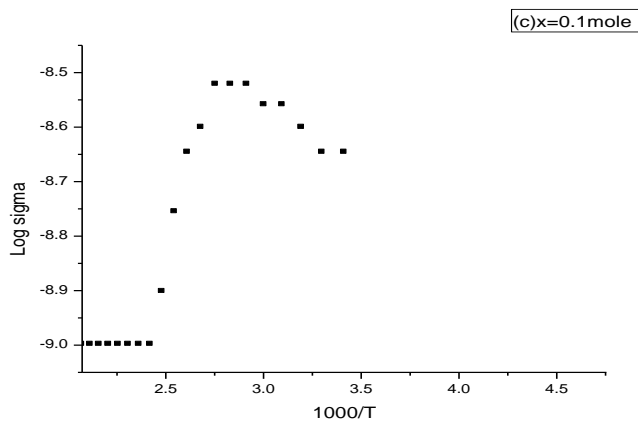

Fig.(5b): Variation of DC- electrical conductivity as a function of temperature for (b) $Bi_2SrV_{1.95}Zr_{0.05}O_9$.

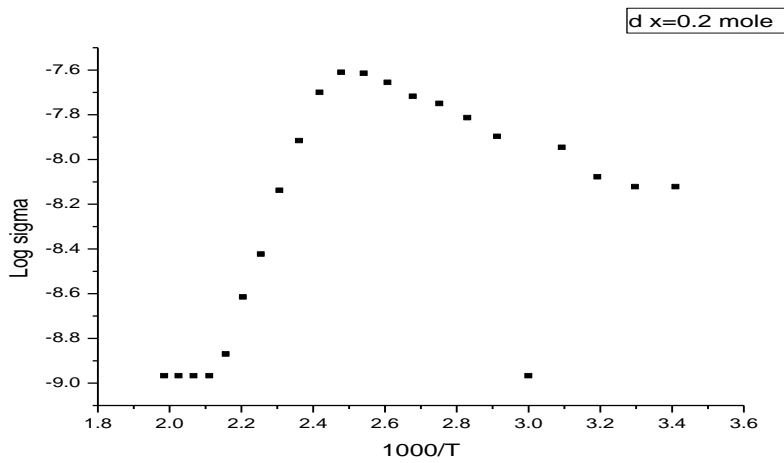**Fig.(5c): Variation of DC- electrical conductivity as a function of temperature for (c) $Bi_2SrV_{1.9}Zr_{0.1}O_9$.**

Fig.(5$_d$): Variation of DC- electrical conductivity as a function of temperature for (d) Bi$_2$SrV$_{1.8}$ Zr $_{0.2}$O$_9$.
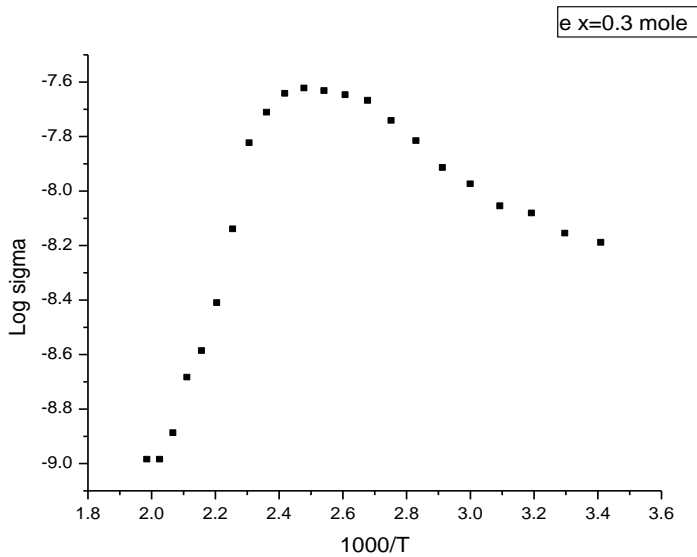
Fig.(5$_e$): Variation of DC- electrical conductivity as a function of temperature for (e) Bi$_2$SrV$_{1.7}$ Zr $_{0.3}$O$_9$.
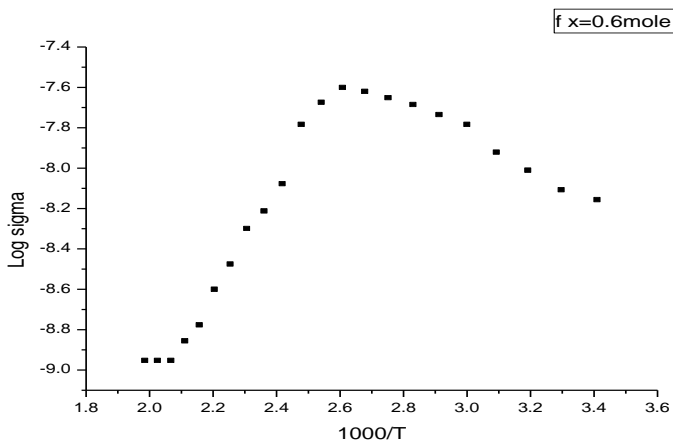
Fig.(5$_f$): the variation of DC- electrical conductivity as a function of temperature for (f) Bi$_2$SrV$_{1.6}$ Zr $_{0.4}$O$_9$
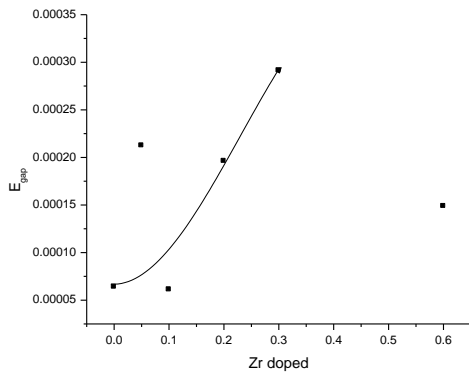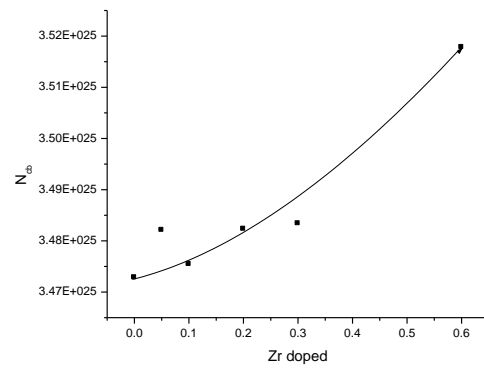
Fig.(6a): Variation of Egab versus Zr –content   **Fig.(6b): Variation of Ncb versus Zr –content**

Fig.(6a,b) show the relation between the energy gap (Eg), number of e- in conduction band (Ncb) for Zr doped in which the Eg and Ncb increase as the ratio of Zr doping increases from x = 0.05 till x = 0.6 mole .

$\rho = \rho_o \ e^{-\Delta Eg/KT}$…………..….. (Eq.1)
$N_{cb} = AT^{3/2} \ e^{-Eg/2KT}$….………(Eq.2)

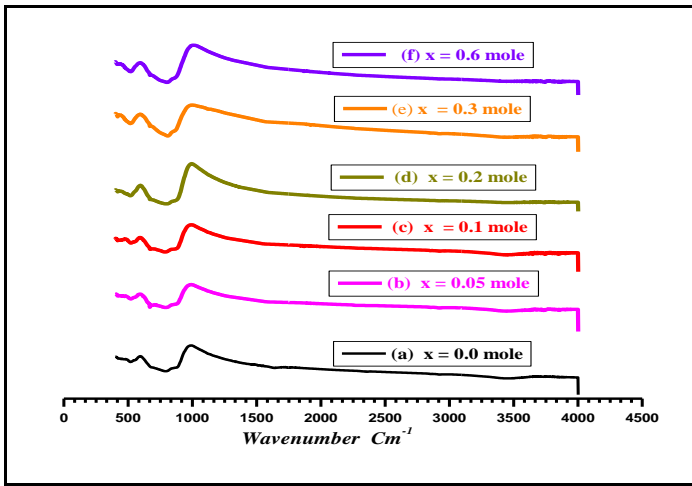**Solid infrared absorption spectral measurements:**

Fig.(7): The room temperature solid infrared absorption spectra recorded for (a): pure Bi$_2$SrV$_2$O$_9$, (b): Bi$_2$SrV$_{1.95}$Zr$_{0.05}$O$_9$,(c): Bi$_2$SrV$_{1.9}$Zr$_{0.1}$O$_9$, (d):Bi$_2$SrV$_{1.8}$Zr$_{0.2}$O$_9$, (e):Bi$_2$SrV$_{1.7}$Zr$_{0.3}$O$_9$, (f):Bi$_2$SrV$_{1.4}$Zr$_{0.6}$O$_9$

The infrared absorption spectra of pure Bi$_2$SrV$_2$O$_9$ and their Zr doped in the range of 500-2500 cm^{-1} are shown in Fig (7).

It is well Known that 212-Bi-Sr-V-O$_9$±ƃ system is mainly belongs to deficient perovskite structure and extra oxygen atom (O$_9$± ƃ). Oxygen nine converts it to distorted perovskite structure and consequently the common vibrational modes of IR-spectra of perovskite are clearly appear.

From Fig.(7) we can summarize the different vibrational modes and their reasons as follows;

1. The range from 400-600 cm^{-1} includes the most of infrared active phonons involving stretching modes of vibrating Bi-O, Sr-O and V-O/Zr-O plus bending modes of Bi-O-V, Bi-O-Sr, respectively.
2. The Broad band around 800 cm^{-1} is mainly due to an increase in the free carrier scattering as reported in [34-35].

3. The vibrational modes at $\approx$ 700-800 cm^{-1} is due to the effect of charge exchangrment of V^{+5}/Zr^{+4} carriers which is enhanced by increasing Zr-dopings.

Conclusions:

In summary, 212-BiSrVO ceramics with various Zr-doping ratios were prepared by the solid state reaction method. X-ray diffraction proved that the compounds have distorted perovskite structure with hexagonal crystal form and the Zr substitution are successfully even at high concentration x= 0.6 mole. The ferroelectric properties of the layered perovskite have been significantly enhanced with Zr doping. The DC-electrical show conducting and semiconducting behavior. The IR spectra displays that the system is belongs to deficient perovskite structure with extra oxygen atom ($O_9\pm\delta$).

References

1. C. A. P. de Araujo, J. D. Cuchiaro, L. D. McMillan, M. C. Scott, and J. F. Scott. Nature (London),374, P. 627–29 (1995).
2. J. F. Scott and C. A. P. de Araujo, Science, 246, P.1400–1405 (1989).
3. G. Z. Cao, pp. 86–112 in Advances in Materials Science and Application*s*. Edited by D.L.Shi. Tsinghua University Press and Springer-Verlag, Beijing, China, 2001.
4. J. F. Scott, p. 115 in Thin Film Ferroelectric Materials and Devices. Edited by R. Ramesh. Kluwer, Norwell, MA, 1997.
5. J. F. Scott, "High Dielectric Constant Thin Films for Dynamic Random Access Memories (DRAM)," Ann. Rev. Mater. Sci., 28, P.79–100 (1998).
6. P. Duran-Martin, A. Castro, P. Millan, and B. Jimenez, J. Mater. Res. 13, P. 2565 (1998).
7. Y. Torii, K. Tato, A. Tsuzuki, H.J. Hwang, and S.K. Dey, J. Mater. Sci. Lett. 17,P. 827 (1998).
8. H. Watanabe, T. Mihara, H. Yoshimori, and C.A.P. Araujo, Jpn. J. Appl. Phys. 34, P. 5240 (1995).
9. J.shimoyama, J.Kasa, T.Morimoto, J. Mizusaki, H.Tagawa, Physica C185-189 P.931 (1981).
10. E. Diaz-Valdes, G. Pacheco-Malagon, G. Contreras-Puente, C. Mejia, -Garcia, G. Andrade-Garay, J. Ortiz-Lopez, A.Conde-Gallardo, C. Falcony,Mater.Chem.Phys. 36, P.64 (1993).
11. K.C. Hewitt, X.K.Chen, X. Meng-Burany, A.E. Curzon, J.C. Irwin, Physica C251, P.192(1995).
12. B. Aurivillius, Arkiv For Kemi, 1(58), P.499-512 (1949).
13. B. Aurivillius, Arkiv For Kemi, 1(54), P.463-80 (1949).
14. B. Aurivillius, Arkiv For Kemi, 2(37), P.519 (1950).
15. T. Rentschler, Materials Research Bulletin, 32(3), P.351-69 (1997).
16. T. Motohashi, Y. Nakayama, T. ujita, K. Kitazawa, J. Shimoyama, K. Kishio, Phys. Rev. B59, P.1408 (1999).
17. J. Shimoyama, Y. Nakayama, K. Kitazawa, K. Kishio, Z. Hirio, I. Chong,M. Takano, Physica C281, P.69 (1997).
18. W.D. Wu, A. Keren,L. P. Le, B.J. Sternlieb, G. M. Luke, Y. J. Uemura, Phys. Rev. B47, P.8127 (1993).
19. Q.Z. Ma, G.H. Ca, Y. Li, N. Chen, China J. Low. Temp. Phys. 18, P.246 (1996).
20. Q.Z. Ma, X.Q. Huang, X.T. Xiong, Y. Li, G.H. Cao, T.B. Zhang, China J. Low Temp. Phys. 19, P.128 (1997).
21. V. Shrivastava, A.K. Jha, R.G. Mmendiratta, Physica B 371, P.337(2001).
22. R.R. Das, P. Bhattacharya, W. Perez, R.S. Katiyar, Ceram. Int. 30, P.1175(2004).
23. C.A.P. de Araujo, L.D. Mc Millan, J.D. Cuchiaro, M.C. Scott and J.F. Scott, Fatigue-free ferroelectric capacitors with platinum electrodes, Nature (London) 374 (6523), p. 627–629 (1995).
24. J.F. Scott and C.A.P. de Araujo, Ferroelectric memories, Science 246(4936), p. 1400–1405 (1989).
25. B. Aurivillius, Structures of Bi_2NbO_5F and isomorphous compounds, Ark. Kemi. 5 (1952), p. 39–47.
26. E.C. Subbarao, Ferroelectricity in $Bi_4Ti_3O_{12}$ and its solid solutions, Phys. Rev. 122(3), p. 804–807 (1961).
27. I. Coondo, A.K. Jha, Solid state Communications 142, P.561-565 (2007).
28. J. Qiu, G.Z. Liu, M. He, H.S. Gu, T.S. Zhou, Physica B 400, P.134-136 (2007).
29. I.coondoo, A.K.Sha, S.K.Aggawal, N.C.Soni, J.electroceram.16, P. 393 (2006).
30. Y. Wu, G. Cao, J. Mat. Res., P.15 (2000).
31. I.Onyszkieuicz, P.Czarnecki, R.Mienas, S.Robaszkiewiez, Physica, (B-C) 147, (2-3), P.166 (1979).
32. T.Hidaka, Phys. Rev. B20, P.2769 (1979).

33. A.Simpson, E.Robert; "Introductory Electronics for Scientists & Engineers", 2nd Edition, allyn and Bacon (1987).
34. A.Memon, M.Khan and SAdallal; Physica C9, P.235-240 (1994).
35. P.Qurong, X.Gao Jie, Z.Zengming and D.Zejum, C70, P. 269-274 (2002).

*****